IET Journals
The Institution of Engineering and Technology

Experimental Evaluation of 30 MHz Band Implant Communication Using Automatic Equalization Technique

ISSN 1751-8644
doi: 0000000000
www.ietdl.org

Kohei Nomura[1], *Daisuke Anzai*[1], *Jianqing Wang*[1]

[1] *Graduate School of Engineeing, Nagoya Institute of Technology, Nagoya, 466-8555, Japan*
✉ *E-mail: wang@nitech.ac.jp*

Abstract: Wireless body area communication technology is attracting much attention in healthcare and medical applications. For reliable and high-speed implant transmission, we previously developed an in-body transceiver at around 30 MHz. However, as the distance between the transmit antenna and the receive antenna gets longer, its bit error rate (BER) performance gets deteriorated. This is because that an implant channel can cause severe waveform distortion and consequent inter-symbol interference (ISI). Meanwhile, equalizing technique provides a powerful means to counteract ISI. In this study we developed an automatic equalizer for the 30 MHz band implant communication. Moreover, we implemented the equalizer on a field programmable gate array (FPGA) board, and evaluated the BER performance with a biological-equivalent liquid phantom. The measurement result shows that our developed equalizer can significantly improve the communication performance in the implant channel.

1 Introduction

Wireless body area communication technology is drawing great attention in the fields of medical treatment and healthcare. Generally, it can be classified into two categories: on-body communication and in-body or implant communication [1]. One typical application of implant communication is capsule endoscope to deliver real-time image/video of small intestine. Capsule endoscopes usually employ 400 MHz band with narrow-band modulation schemes and their data rate is limited to several hundred kbps [2]. From the perspective of implant applications, a data rate as high as several Mbps is strongly required at a high reliability. One attempt has been made to employ ultra wide band (UWB) low band to improve the communication speed, but it suffers from the very large signal attenuation inside the human body [3]. Therefore, we newly proposed to employ the extremely weak radio band at 10∼60 MHz as a promising candidate of physical layer for implant communication [4][5]. This is because the 10∼60 MHz band exhibits less propagation loss in the human body compared to the higher frequency bands. Moreover, the use of wideband impulse radio (IR) modulation makes it possible to communicate with high speed and low power consumption. In our previous study, we have developed an impulse radio - on off keying (IR-OOK) transceiver using register transfer level (RTL) design tool on a field programmable gate array (FPGA) board, and evaluated the bit error rate (BER) performance of the transceiver with a biological-equivalent liquid phantom. However, as will be shown later in Section 2, the implant communication channel can cause serious waveform distortion and consequent inter-symbol interference (ISI). As the distance between the transmit antenna and the receive antenna got longer, the BER performance was found to get deteriorated. In view of the effectiveness of equalizing technique in mitigating ISI, we aim to newly develop an automatic equalizer in our transceiver in this study for further improving the performance of our 30 MHz band transceiver.

2 Transceiver Structure and ISI Mitigation

Fig. 1 shows the block diagram of the in-body IR transmitter whose specifications are shown in Table 1. The digitized image/video signals are modulated with short pulses based on IR scheme in the transmitter. A pulse generator is used to produce pulses to be transmitted with a width of 10 ns and a repetition period of 104 ns. In order to transmit the digitized information bits, we use the pulse to represent "1", and nothing to represent "0". The modulated pulse trains are spectrum-formed by a band pass filter (BPF) of 10∼60 MHz at the transmitter output as well as the band-pass features of the transmit/receive antennas. These antennas were designed in a hollow cylinder shape with dimensions of 12 mm × 12 mm × 20 mm by forming the radiation elements on a flexible magnetic sheet [5]. Table 2 summarizes the specifications of the transmit and receive antennas. The transmitter was implemented in a field programmable gate array (FPGA, Xilinx Sparian-6) board with dimensions of 35 mm × 45 mm. The circuitry can be integrated into an IC chip so that its size is sufficiently small to be inserted in the hollow cylinder shape antenna as a capsule.

We measured the received signal which passed through a biological equivalent liquid phantom in place of actual human body. In order to simulate the implant channel, it is necessary to make the dielectric properties of the liquid phantom as close as possible to that of

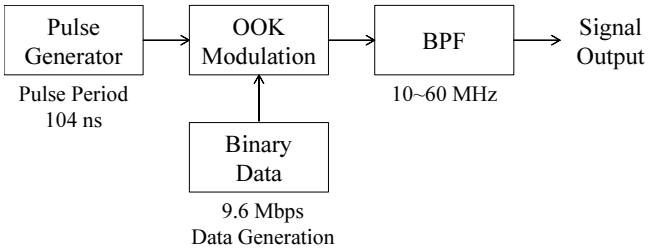

Fig. 1: Block diagram of the in-body IR transmitter

Table 1 Specifications of the in-body IR transmitter

Parameter	Value
Transmit Power	-4.1 dBm (at 30 MHz)
Pulse Width	10 ns
Bandwidth after Front-End Processing	50 MHz
Repetition Period of Pulse	104 ns
Bit Rate	9.6 Mbps
Length of Pilot Signal	32 chips
Forward Error Correction	None

Table 2 Specifications of transmit and receive antennas

Parameter	Value
Dimensions	12 mm × 12 mm × 20 mm
Resonance frequency	30 MHz
-10 dB bandwidth	2.2 MHz
Gain	-45 dBi

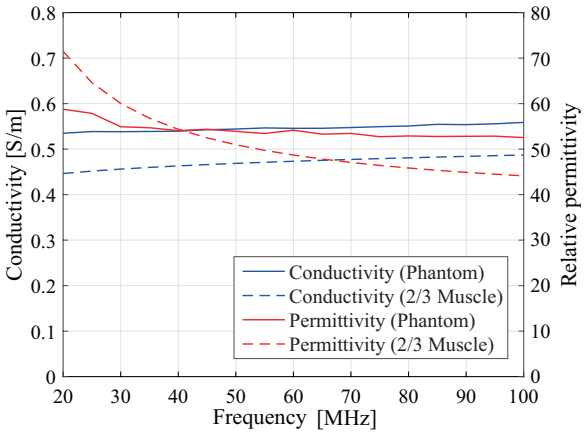

Fig. 2: Measured conductivity and relative permittivity of the liquid phantom

the human body. Due to the difficulty in making a heterogeneous phantom to simulate various human organs, it should be reasonable to employ a homogeneous phantom to simulate an average dielectric property of human body. The average dielectric property is usually considered as the muscle's one with a scaling factor of 2/3, i.e., the so-called 2/3-muscle. Fig. 2 shows the relative permittivity and conductivity of a commercially available liquid phantom [6]. They were measured from 20 MHz to 100 MHz by using a dielectric assessment kit (Speag, DAK). As can be seen from Fig. 2, the relative differences between the liquid phantom and the 2/3-muscle are 10% for permittivity and 17% for conductivity at 30 MHz. In view of that the liquid phantom exhibits a dielectric property close to the 2/3-muscle, as the first step, we therefore employ the liquid phantom, in place of the actual human body, to evaluate the validity of our developed equalizer. Fig. 3 shows the measurement environment of the received signal. The transmit antenna was inserted in the liquid phantom and connected to the transmitter. The modulated pulse waveform at the transmitter output was then measured by using an oscilloscope.

Fig. 4 shows an example of the time waveform of transmitted signal at the transmitter output. As we mentioned in the previous section, an implant channel can cause severe waveform distortion. Fig. 5 shows the received signal waveform at the input of receiver (after the receive antenna). Compared to Fig. 4, we can confirm that the received signal in Fig. 5 is indeed obviously influenced by ISI due to the signal propagation in the human body. To overcome the ISI, it is valid to introduce an equalizer in the receiver for the implant channel.

3 Equalizer and Receiver Structure

There are two typical linear equalizers: the minimum mean-square error (MMSE) equalizer and the zero-forcing (ZF) equalizer. The former minimizes the expected mean-squared error between the transmitted symbol and the symbol detected at the equalizer output, thereby providing a great ISI mitigation and noise reduction effect. The latter cancels all ISI but can lead to larger noise enhancement. Compared to the MMSE algorithm, the ZF algorithm has a significantly reduced complexity [7]. Since a capsule endoscope requires to be miniaturized and has low energy consumption, we adopted

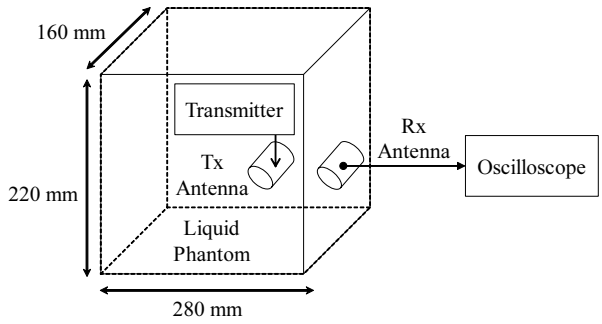

Fig. 3: Measurement environment of the received signal

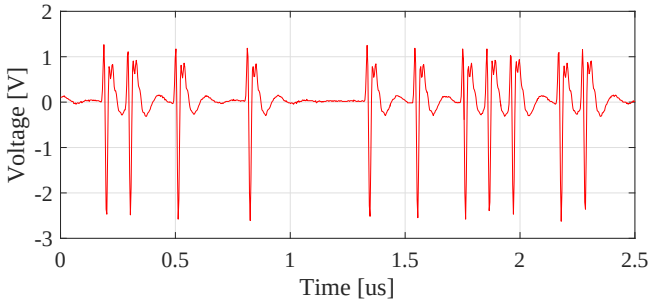

Fig. 4: Example of time waveform of transmitted signal

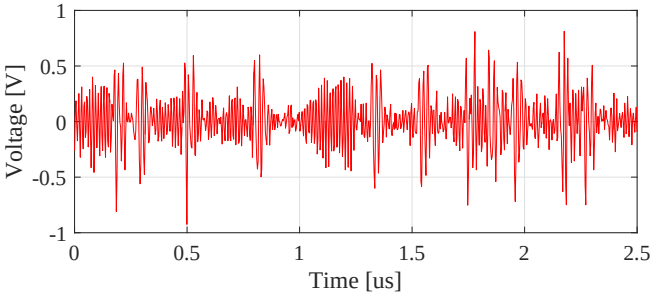

Fig. 5: Example of time waveform of received signal

the ZF algorithm to reduce the circuit scale for the implant channel equalization.

3.1 *Zero-Forcing Algorithm*

The ZF equalizer forces the receiver output to be zero at all the sampling instances, except for the time instant which corresponds to the transmitted pulse. This can be accomplished by a finite impulse response (FIR) filter [8]. The output of the equalizer $y(kT)$ is expressed as the discrete convolution of the input signal $x(kT)$ and the equalizer filter coefficient $c(nT)$:

$$y(kT) = \sum_{n=-N}^{N} c(nT) \cdot x[(k-n)T] \tag{1}$$

where k is the sample number of the discretely sampled signal, and T is the tap spacing of the equalizer. Using a more convenient notation y_k to denote $y(kT)$, c_n to denote $c[nT]$, and x_{k-n} to denote $x[(k-n)T]$, Eq. (1) can be expressed as

$$y_k = \sum_{n=-N}^{N} c_n \cdot x_{k-n}. \tag{2}$$

The ZF equalizer requires the samples $y_k]0$ for $k \neq 0$, and $y_k = 1$ for $k = 0$. Substituting these values into Eq. (2), we obtain a set of simultaneous equations of $2N + 1$ variables. Clearly, it is impossible to solve the set of simultaneous equations. However, if we specify the values of $y[k]$ only at $2N + 1$ points as

$$y_k = \begin{cases} 1 & k = 0 \\ 0 & k = \pm 1, \pm 2, \cdots, \pm N \end{cases} \tag{3}$$

then a unique solution exists, and x_n meeting the above condition actually corresponds to the channel impulse response h_n. This assures a pulse having zero interference at the sampling instants of N preceding and N succeeding pulses. Because the pulse amplitude decays rapidly, interference beyond the N_{th} pulse is not significant for $N > 2$. Substitution of the condition (3) into Eq. (2) yields a set of $2N + 1$ simultaneous equations of $2N + 1$ variables:

$$\begin{bmatrix} 0 \\ \vdots \\ 1 \\ \vdots \\ 0 \end{bmatrix} = \begin{bmatrix} h_0 & h_{-1} & \cdots & h_{-2N} \\ \vdots & \vdots & & \vdots \\ h_N & h_{N-1} & \cdots & h_{-N} \\ \vdots & \vdots & & \vdots \\ h_{2N} & h_{2N-1} & \cdots & h_0 \end{bmatrix} \begin{bmatrix} c_{-N} \\ \vdots \\ c_0 \\ \vdots \\ c_N \end{bmatrix} \tag{4}$$

The filter coefficient c_n can be obtained by solving this set of equations [9] based on estimated impulse response h_n.

3.2 Derivation of Filter Coefficients

It is necessary for the ZF equalization to estimate the channel impulse response first. In this study, we implemented an automatic equalizer which renews the filter coefficients automatically. The designed equalizer estimates the channel transfer function from the transmitted/received signals, and derives the impulse response by computing the inverse fast Fourier transform (IFFT) of the transfer function. To obtain the transfer function, we employed a known signal sequence as the training signal for the equalizer. The training signal was a random "1" and "0" sequence of 252 bits, which is arranged between the start bits and the stop bits. First, the transmitter transmits the training signal regularly, and the equalizer in the receiver determines the training signal from the received signal. Next, the equalizer calculates the frequency spectra of the transmitted and received training signals by using the fast Fourier transform (FFT) respectively. Subsequently, the channel transfer function $H(f)$ is derived from the transmit frequency spectrum $T_x(f)$ and the receive frequency spectrum $R_x(f)$ as

$$H(f) = R_x(f)/T_x(f). \tag{5}$$

Furthermore, the equalizer computes the IFFT of the transfer function $H(f)$ and obtains the impulse response $h(t)$ (or h_n). Finally, the equalizer derives the filter coefficients of the equalizer from Eq. (4) with the estimated channel impulse response. It should be noted that the update of filter coefficients c_n can be renewed in an interval smaller than 20 μS. With the movement of the in-body transceiver, the FIR filter coefficients are renewed regularly by the ZF algorithm. Since the movement speed of an in-body transmitter is usually very slow inside the human body, frequency updates of filter coefficients are not necessary. In this sense, we consider the equalizer as an automatic one because it regularly monitors the implant channel based on the training signal and renews the filter coefficients if necessary.

3.3 Receiver Structure and Simulation

We implemented the FIR filter whose coefficients were derived in the previous subsection using RTL design tool, and performed a simulation on the developed equalizer by using Xilinx ISim (Hardware description language simulator) to evaluate its performance. First, we converted the received signal in Fig. 4 to 10 bit quantized signal. We therefore showed each of the following FIR filter output values not in the unit of voltage but analog to digital converter (ADC) output. Fig. 6 shows the equalized signal when the signal shown in Fig. 5 was input to the equalizer. Moreover, we extracted the envelopes of the received signal as shown in Fig. 7 and the equalized signal as shown in Fig. 8. It is evident that the designed equalizer mitigates the ISI and improve the signal quality by comparing Fig. 7 and Fig. 8. To evaluate the effectiveness of the equalization quantitatively, we calculated the correlation coefficients between the received or equalized signal and the transmitted signal. Fig. 9 shows the correlation coefficients at different communication distances. The communication distance indicates the separation between the center of the implant antenna and the center of the receiving antenna. This figure indicates that the correlation coefficients of the equalized signal were improved significantly at all of the communication distances. Therefore, our equalizer is effective to mitigate the ISI and reduce the waveform distortion in implant communication.

We then installed the designed equalizer in the receiver implemented on an FPGA evaluation board (Xilinx, Virtex-6 ML605). Fig. 10 shows the block diagram of the receiver. The receiver employs an envelope detector for demodulation. At the beginning, the quantized received signal is filtered and sent to the equalizer to mitigate ISI. Subsequently, the envelope extraction unit extracts the envelope of the equalized signal. After the envelope detector, the signal is

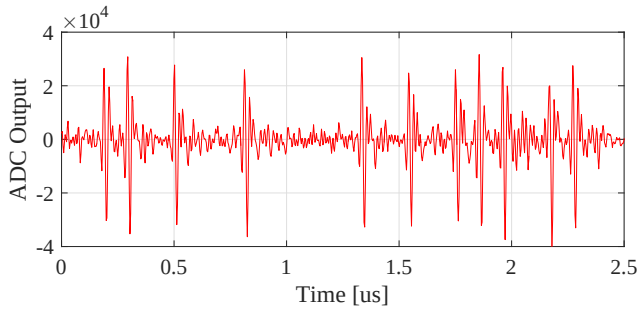

Fig. 6: Example of time waveform of equalized signal

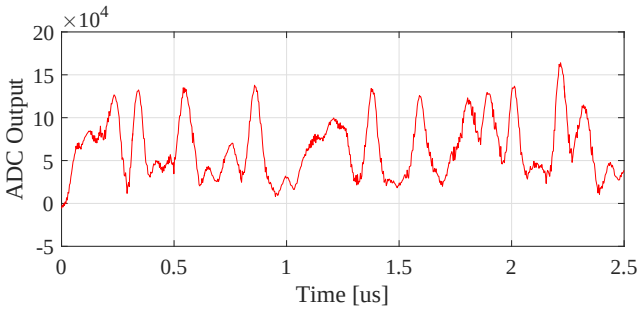

Fig. 7: Envelope of time waveform of received signal

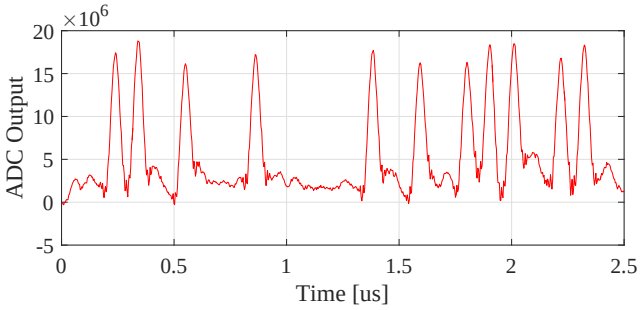

Fig. 8: Envelope of time waveform of equalized signal

Table 3 Hardware requirement and convergence time of the FPGA-implemented equalizer

Parameter	Value
Number of slice registers	8242
Number of slice look up tables	7724
Operating clock frequency	156.25 MHz
Convergence time of filter coefficient derivation	17.6 μS

Table 4 Sensitivity of filter coefficients of equalizer

Parameter	Variation (RMSE)
Dielectric property variation by 10%	0.31
Communication distance: 6 cm vs. 12 cm	0.31
Implant antenna orientation: Parallel vs. perpendicular	0.29

judged as "1" or "0" by a comparator. Finally, these digitized data are transmitted to a PC via a USB port.

Table 3 shows the hardware requirement and convergence time of the FPGA-implemented equalizer.

4 Communication Performance Evaluation

4.1 Pre-investigation for Phantom Experiment

Before the experimental performance evaluation of implant communication, we first investigated the validity of the experiment setup, especially for the use of a coaxial cable used to connect the implant antenna and the transmitter. Fig. 11 shows the view of phantom experiment where a coaxial cable was used or not. In the case that the coaxial cable was not used, an SMA adapter was used to directly connect the implant antenna to the transmitter. Fig. 12 compares the BER performances in the two cases. In the case with the coaxial cable, the BER versus the communication distance, i.e., the separation between the center of the implant antenna and the center of the receiving antenna, was better as compared with the case without the coaxial cable. In the latter case, the BER was larger than 0.1 when the communication distance exceeded 150 mm. Since such a BER level did not suggest any meaning communication, we did not show them for a distance larger than 150 mm in Fig. 12. This finding may be attributed to that the transmit signal was radiated also from the coaxial cable so that the received signal at the receive antenna was greater than the actual one in the case with the coaxial cable. It should be noted that although the coaxial cable was covered with ferrite cores as shown in Fig. 11, this difference on BER performance was still so obvious. This result indicates that, in the performance evaluation of implant communication, it is essential to connect the transmit antenna directly to the transmitter without using a coaxial cable.

In addition, we also investigated how sensitive the equalizer is with respect to the dielectric properties of biological tissue, communication distance as well as antenna orientation. We changed the dielectric properties by 10% for biological-equivalent liquid phantom, the communication distance from 6 cm to 12 cm, and the implant antenna from parallel orientation to perpendicular orientation. To quantitatively show their influences to the equalizer, we calculated the root mean squared error (RMSE) of the FIR filter coefficients of equalizer, as an index of corresponding variation, when we changed the above parameters. Table 4 shows the RMSE of filter coefficients, which suggests that the equalizer is quite sensitive with respect to the tissue types, communication distance and antenna orientation, and regular updating of filter coefficients is necessary.

4.2 BER Performance Evaluation

To clarify the communication performance of our developed equalizer, we evaluated the BER performance in a biological-equivalent liquid phantom. Fig. 13 shows the measurement setup. We connected the transmit antenna directly to the transmitter and the receive antenna directly to the receiver. The transmitter together with the transmit antenna was inserted in the liquid phantom. This makes the measurement setup effectively simulating an implant communication situation because possible radiation from the coaxial cable between the transmit antenna and the transmitter did not exist. To prevent the transmitter and antenna from directly touching the liquid, they were wrapped with vinyl. On the other hand, the receive

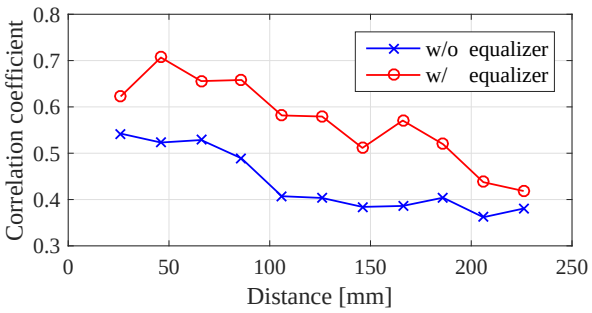

Fig. 9: Correlation coefficients at different communication distances

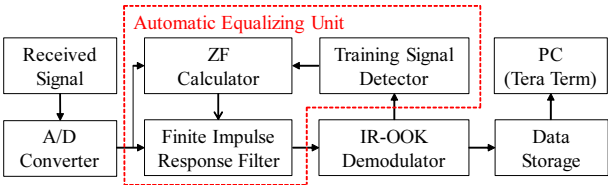

Fig. 10: Block diagram of the developed receiver

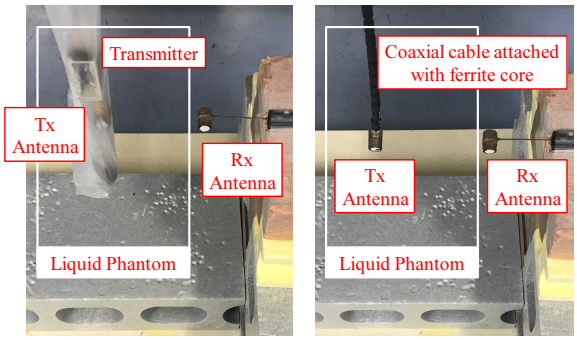

(a) w/o coaxial cable (b) w/ coaxial cable

Fig. 11: View of the coaxial cable experiment

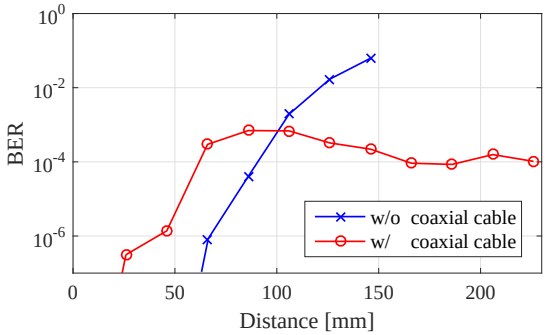

Fig. 12: BER performance with coaxial cable or not

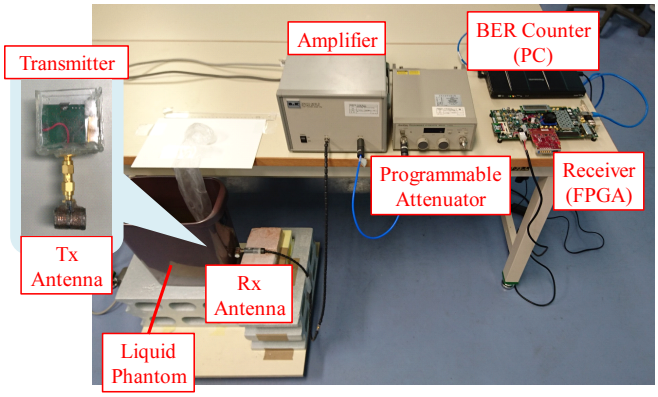

Fig. 13: View of the phantom experiment setup

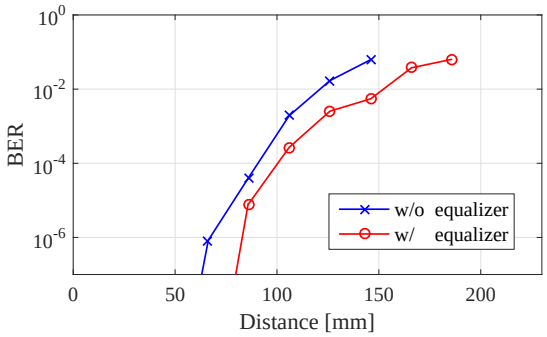

Fig. 14: BER performance versus communication distance

antenna and the receiver were set at the phantom surface with a 5 mm spacing. The data to be transmitted for BER measurement were produced in the transmitter by a pseudo-noise (PN) sequence generator, and the receiver was connected to a PC via USB interface for recording the received data and counting the BER.

Fig. 14 shows the measured BER performance as a function of distance from the implant antenna to the phantom surface at a data rate of 9.6 Mbps. As can be seen, the BER performance with the automatic equalizer is totally improved by one digit and the communication distance is significantly extended as compared to before. As a result, in the biological-equivalent liquid phantom, we have accomplished a BER smaller than 10^{-2}, which is an acceptable BER level in the physical layer, at an implant communication distance up to 15 cm for the data rate as high as 9.6 Mbps.

Moreover, we also evaluated the communication performance if we employed the direct sequence spread spectrum - IR (DSSS-IR) modulation for further improving the BER performance instead of sacrificing the data rate. We measured the BER performance for various spreading ratios, in other words, different data rates. In the DSSS-IR modulation, the binary data were encoded by a PN sequence having the spreading ratio $L = 1 \sim 8$ which corresponds the data rate from 9.6 Mbps to 1.2 Mbps. Fig. 15 shows the BER performance with the equalizer as a function of spreading ratio $L = 1 \sim 8$. As a result, the BER was obviously improved with the decrease of data rate, and a BER of 10^{-2} was secured up to nearly 20 cm inside the human body at a data rate of 2.4 Mbps. This can also confirmed from Fig. 16 which shows the BER performance with the equalizer whose spreading ratio $L = 1 \sim 8$ as a function of the communication distance. It is clear from Fig. 16 that the developed receiver with the equalizer has indeed achieved a reliable implant communication distance of at least 18.6 cm at the spreading ratio $L = 4$ (2.4 Mbps). These experimental results sufficiently demonstrate a largely improved communication performance at a high transmission speed and deep communication distance by using of the developed automatic equalizer.

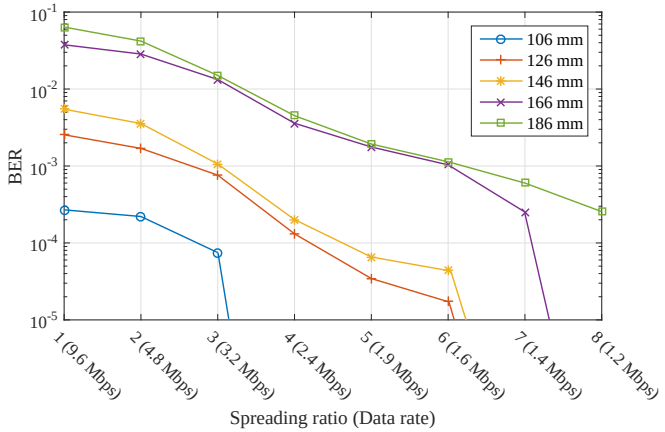

Fig. 15: BER with the equalizer versus spreading ratio L or data rate

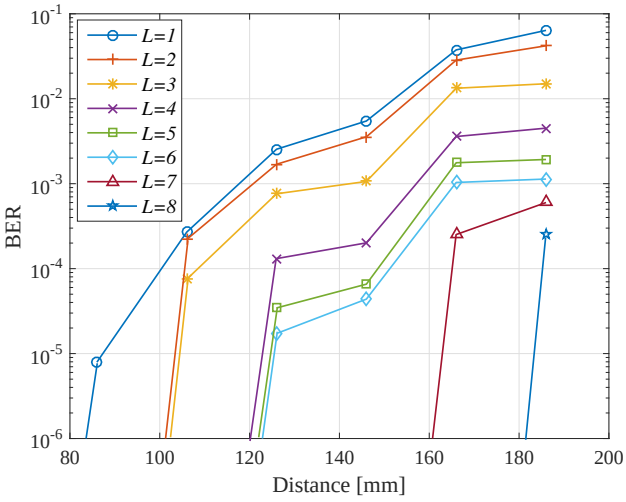

Fig. 16: BER with the equalizer versus communication distance

5 Conclusion

High quality image/video transmission requires a high data rate at Mbps order in wireless implant communications. To satisfy this requirement, we previously developed an in-body IR transceiver with a small-size implant antenna at 30 MHz. In view of that an implant communication channel causes significant waveform distortion to result in a serve ISI, in this study, we developed a ZF equalizer for the implant channel and implemented the equalizer in the FPGA-based receiver. Moreover, we evaluated its BER performance with a biological-equivalent liquid phantom. The measurement results have demonstrated a BER smaller than 10^{-2} in the physical layer in a depth of at least 15 cm with a date rate of at least 9.6 Mbps, and nearly 20 cm with a date rate of at least 2.4 Mbps. This performance sufficiently shows the feasibility and usefulness of our developed receiver with the equalizer for high-speed implant communication such as in capsule endoscopes.

The future subject is to conduct experimental validation with living animal.

6 Acknowledgments

This study is supported in part by the Strategic Information and Communications R&D Promotion Programme (SCOPE), Ministry of Internal Affairs and Communications, Japan.

7 References

[1] J. Wang, and Q. Wang, Body Area Communications, Willey-IEEE, 2012.
[2] M. R. Yuce, and T. Dissanayake "Easy-to-swallow wireless telemetry," IEEE microwave magazine, vol.13, no.6, pp.90-101, Sep.-Oct. 2012.
[3] D. Anzai, K. Katsu, R. Chavez-Santiago, Q. Wang, D. Plettemeier, J. Wang and I. Balasingham, "Experimental evaluation of implant UWB-IR transmission with living animal for body area networks," IEEE Trans. Microwave Theory Tech., vol.62, no.1, pp.183-192, Jan. 2014.
[4] H. Narita, D. Anzai, and J. Wang, "Experimental evaluation of wide band implant communication at 30MHz band," IEICE Technical Report, MICT2014-73, pp.7-12, Mar. 2015 (in Japanese).
[5] J. Wang, J. Liu, K. Suguri and D. Anzai, "An in-body impulse radio transceiver with implant antenna miniaturization at 30 MHz," IEEE Microw. and Wireless Comp. Lett., vol.25, no.7, pp.484-486, July 2015.
[6] Body Tissue Dielectric Parameters [Online]. Available: https://www.fcc.gov/general/body-tissue-dielectric-parameters
[7] A. Goldsmith, Wireless Communications, Cambridge University Press, 2005, pp.351-359.
[8] S. Haykin, Adaptive Filter Theory, 3rd ed., Prentice Hall, 1996, pp.217-220.
[9] B. P. Lathi and Z. Ding, Modern Digital and Analog Communication Systems, 3rd ed., Oxford University Press, 1998, pp.323-325.